RSC Advances

PAPER

View Article Online
View Journal | View Issue

Cite this: *RSC Adv.*, 2021, **11**, 26635

Enhancing catalytic potential of gold nanoparticles by linear and cross-linked polyurethane blending

Amna Murtaza,[a] Maliha Uroos,*[a] Misbah Sultan,[b] Rabia Muazzam[a] and Sadia Naz[a]

This work describes the synthesis of gold nanoparticles (AuNPs) and their subsequent stabilization using a water-borne polyurethane matrix of micro-particles (Au/PU) by a heating method. Composites were prepared both from linear and cross-linked polyurethane (LPU and CPU). Catalytic activities of synthesized composites exhibiting 226.4 nm size were evaluated for reduction of Congo red dye. More than 90% Congo red degradation was achieved in just 6 minutes with Au/LPU. Under similar conditions, 30% of dye was degraded with Au/CPU composite in 5 minutes. The effects of different variables such as concentration of dye, catalyst dose and concentration of reagents have been optimized. The degradation process followed first order kinetics. The most efficient composite (Au/LPU) was characterized using UV/Vis, FTIR, SEM, XRD and DLS techniques. The excellent catalytic activity can be attributed to the polyurethane matrix making the dye available to catalytic sites (AuNPs).

Received 16th June 2021
Accepted 23rd July 2021

DOI: 10.1039/d1ra04662d

rsc.li/rsc-advances

1. Introduction

Environmental nanotechnology is playing an influential role in upgrading environmental engineering and science due to its wide applications in various environmental concerns such as contaminants detection, adsorptive removal and catalytic degradation.[1] Gold nanoparticles (AuNPs), in this context, have attracted substantial consideration in numerous frontline arenas including biomedicines,[2] immobilization of biomolecules,[3] smart materials,[4] electronics,[5] solar cells,[6] sensing,[7] catalysis[8] and in DNA sequencing.[9] Due to their large surface area-to-volume ratio, the catalytic activities are superior to any other bulk metal. The only downside in using these nanoparticles (NPs) alone is that they are unstable and aggregate in solution owing to their high surface energies, due to which their catalytic activities are badly affected. So, their stabilities and physicochemical properties are enhanced by immobilizing them on various supports ranging from nano-carriers to inorganic materials and organic polymers.[10]

Research on structural and functional properties of these polymer–metal nanoparticle blends is gaining considerable attention in recent years due to their vast practical and fundamental applications.[11] Nanofibers,[12] nanospheres,[13] titania nanotubes,[14] carbon nanotubes,[15] meso-structured materials,[16] polyurethane,[11] silica,[13] clay,[14] cellulose,[17] graphene[18] and many other materials are well described for the purpose. This immobilization makes the nanoparticles of gold (AuNPs) well dispersed in nanocomposites exhibiting hybrid properties and a stable structure. Surface adsorption and charge transfer properties by this immobilization also facilitate the catalytic efficiencies.[19] From all these, natural polymers are the best option due to their surface chemistry and well-regulated pore space as well as their outstanding mechanical strength for longstanding applications. The consequential polymer-based nanocomposite (PNC) possesses dual intrinsic properties of polymer as well as nanoparticles; nanoparticles are now highly stable with extraordinary process abilities as well as fascinating advances are caused due to nanoparticle–matrix interaction.[1]

In this work, we synthesized AuNPs nanocomposites with waterborne polyurethane (PU) based on the high biological and mechanical properties of PU such as non-toxicity, non-flammability, inexpensive, eco-safe, low viscosity at high molecular weight[20] and wide applicability in cardiovascular biomaterials, synthetic elastomers,[21] leather, textile, glass fibers, wood, paper and others.[11] Previously reported PU are based on polyvinyl alcohol (PVA) polytetramethylene oxide (PTMO),[22] intercalated silicate layers added in PTMO,[23] α-thiethyl, ω-hydroxypoly(*tert*-butyl acrylate),[24] hexamethylene diisocyanate and polyester polyol.[25,26] In this study, we synthesized linear and cross-linked PU polymers from polyethylene glycol (PEG), toluene diisocyanate (TDI) and tetraethylene-pentamine (TEPA) using our previously developed methodology.[27] Redox catalytic potential of stabilized AuNPs on PU polymer matrix were then evaluated by degradation of Congo red dye that is an anionic dye and is released in environment through industrial effluents of textile, paper, rubber and plastic industries.[22] Previous studies revealed that polyurethane (PU) is

[a]*Centre for Research in Ionic Liquids, School of Chemistry, University of the Punjab, 54590, Lahore, Pakistan. E-mail: malihauroos.chem@pu.edu.pk*

[b]*Centre for Applied Chemistry, School of Chemistry, University of the Punjab, 54590, Lahore, Pakistan*

one of the most fascinating synthetic elastomers. When a small amount of AuNPs was added in PU, its thermal and mechanical characteristics as well as stability has been significantly increased.[11] It has been analyzed that AuNPs could incite morphological changes in PU.[26] For estimation of photocatalytic efficiency of polyurethane/TiO_2 nanocomposite, photocatalytic reduction of rhodamine-B has been evaluated. These nanocomposites were also recyclable.[28] Pd catalyst based on chitosan–tannin (CT) framework as support was reported recently. Catalytic efficiency for degradation of Congo red was investigated. The catalyst was effective in degradation of 23% Congo red in 60 min.[29] Cellulose based gold nanocrystals were synthesized and studied for their excellent degradation activities against various dyes.[30] Gold nanoparticles (AuNPs) loaded on polymer resin were synthesized and catalytic efficiency was studied.[31]

2. Materials and methods

2.1 Chemicals and reagents

Tetrachloroauric acid ($HAuCl_4 \cdot 3H_2O$), sodium borohydride ($NaBH_4$), polyethylene glycol (PEG, M_w: 1000 g mol^{-1}), toluene diisocyanate (TDI), Congo red (CR) and tetraethylenepentamine (TEPA) were purchased from Sigma Aldrich and used as such.

2.2 Gold nanoparticles (AuNPs) synthesis

AuNPs were formed *via* chemical reduction of $HAuCl_4 \cdot 3H_2O$ (1 mM solution in water) in the presence of sodium citrate as reported in literature.[32] Firstly, 1 mM solution of $HAuCl_4$ (8 mL) was stirred at 60 °C after that 2 mL of 1% sodium citrate was added at 98 °C. At this temperature, vigorous stirring was provided to the reaction mixture for 10 minutes. Prepared AuNPs were examined through T90, PG Instruments Ltd UV/Vis spectrophotometer.[33]

2.3 Synthesis of Au/LPU and Au/CPU composites

LPU (linear polyurethane) as well as (CPU) cross-linked polyurethane were synthesized from TEPA, TDI and PEG according to our reported method.[27] For composites formation, LPU (0.05 g) was dispersed in the freshly prepared AuNPs (10 mL) solution in a typical procedure. The reaction mixture was heated at 98 °C for 5 min with vigorous shaking. This reaction yielded a colloidal solution of purple Au/LPU composite. The colloidal solution was centrifuged for about 15 minutes at 4000 rpm. The supernatants were decanted off and composite was collected at the bottom. The same procedure was repeated with CPU.

2.4 Characterization techniques

Electronic transitions in the composite were visualized by UV/Vis spectrophotometer in the range of 200–800 nm. Identification of various functional groups in composites was done using FTIR spectrophotometer (Agilent technologies Cary 630 FTIR) in the range of 4000–625 cm^{-1}. Morphology, phase composition was analyzed by Scanning Electron Microscope (SEM, TESCAN Vega LMU). Crystallinity of synthesized NPs in composite was investigated by XRD analysis. Particle size and size distribution was determined by Nano ZS (Malvern Instruments Ltd).

2.5 Reduction of Congo red (CR)

Redox potential of produced nanocomposite was evaluated for Congo red (CR) dye. 1 mL of 1 mM CR was taken with 4 mL of sodium borohydride ($NaBH_4$) (40 mM) and 9 mL of distilled water. Then 0.3 mg Au/LPU composite was added in the above reaction mixture and mixed well. The degradation process of dye was analyzed continuously by UV-Vis spectrophotometer. The same procedure was done for Au/CPU and AuNPs alone (before nanocomposite formation).

2.6 Effect of different reaction parameters on catalytic degradation of CR

Effect of different reaction parameters like concentration of CR dye, $NaBH_4$ and Au/LPU, time, temperature and others was tested by a series of experiments. The effect of each parameter was examined by keeping all other parameters persistent. The detail of different reaction parameters has been shown in Table 1. Percent (%) removal of dye in all typical runs has been evaluated by the general formula given below.

$$\mathrm{Pr} = \frac{C_o - C_t}{C_o} \times 100$$

where Pr is the percent removal of CR, C_o is initial concentration of CR and C_t is the concentration of CR at time t.

2.7 Kinetic study of reduction process

Rate constants and order of reactions were evaluated *via* kinetic analysis of degradation procedure with and without polymer blending. Obtained ln C_t/C_o was plotted against reaction time.

2.8 Recycling and reuse of Au/LPU composite

Reusability of composite was investigated up to five runs. The used composite was separated by centrifugation from reaction mixture, and then applied in next experiment.

Table 1 Various compositions of reaction mixture used to study different parameters of catalytic reduction of CR dye with Au/LPU

Parameters	Congo red (mM)	Au/LPU (mg mL^{-1})	$NaBH_4$ (mM)	Completion time (min)
Au/LPU conjugate	1	0.1	40	7
	1	0.3	40	6
	1	0.5	40	4
$NaBH_4$	1	0.3	30	9
	1	0.3	40	6
	1	0.3	50	3
Congo red	0.5	0.3	40	3
	1	0.3	40	6
	2	0.3	40	13

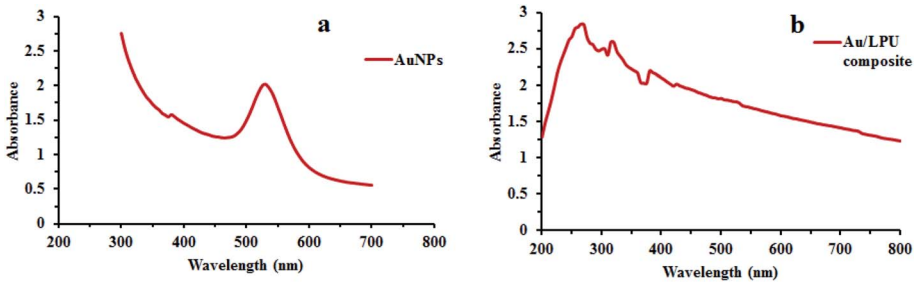

Fig. 1 UV/Vis absorption spectrum of (a) AuNPs and (b) Au/LPU composite.

3. Results and discussion

3.1 UV/Vis analysis

UV/Vis absorption spectrum of synthesized gold nanoparticles (AuNPs) is shown in Fig. 1. The Surface Plasmon Resonance (SPR) band at 530 nm is characteristic of AuNPs. However, disappearance of this characteristic band at 530 nm has been observed by the addition of LPU in AuNPs solution. This indicates strong binding of synthesized AuNPs with LPU.[34] The major binding site was –NH of PU linkage and is evident from FTIR peak shift in Section 3.2.

3.2 FTIR analysis

FTIR analysis was performed to confirm the proposed synthesis of PU and its composite. FTIR spectra of LPU and Au/LPU composite can be seen in Fig. 2. The major bands for the PU formation observed for the –NH stretching vibration at 3419 cm^{-1}, C=O at 1715 cm^{-1} and –NH bending at 1540 cm^{-1}. Other prominent peaks are at 1229 cm^{-1}, 1091 cm^{-1} and 946 cm^{-1} for C–O–C stretching vibrations; 1599 cm^{-1} for aromatic C=C bond and 1636 cm^{-1} is for amide region in LPU.[34,35] By the addition of AuNPs in LPU, the C=O (carbonyl) stretching band exhibited a red shift from 1715 cm^{-1} to 1707 cm^{-1}. A peak at the position of 1707 cm^{-1} has shown hydrogen bonded carbonyl group in composite.[36] These results revealed that the dispersion of AuNPs in the PU matrix resulted in the formation of strong hydrogen bond and carbonyl peaks with different amount of AuNPs (43.5–65 ppm) has been reported recently.[26] Any observable shift in –NH band between 3300–3400 cm^{-1} are mostly associated with hydrogen bond of PU with AuNPs.[37] In the present study, a shift of –NH peak from 3419 cm^{-1} for pure LPU to 3380 cm^{-1} for Au/LPU was also observed with significant broadening.

Similarly, for CPU, appearance of a C=O urethane stretching band at 1636 cm^{-1} with a shoulder near 1715 cm^{-1} reveals the successful synthesis of CPU (Fig. 3). However, for Au/CPU composite, the disappearance of C=O stretching band at 1715 cm^{-1} suggests incorporation of AuNPs in PU.

Moreover –NH band of PU exhibited a red shift from 3437 to 3296 cm^{-1} on addition of AuNPs. These results suggest the engagement of –NH of urethane link with AuNPs leading towards decreased secondary interactions among –NH and C=O of PU chain. Where –NH was the hydrogen-bond donor and C=O was acceptor in urethane linkage.[38]

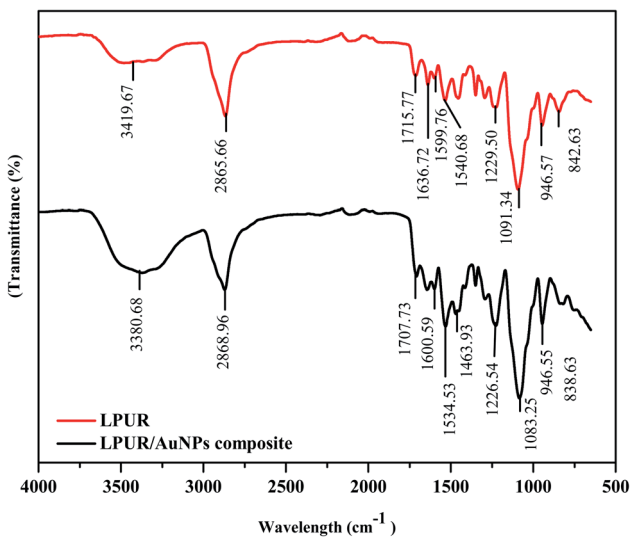

Fig. 2 FTIR spectra of synthesized linear polyurethane (LPU) and Au/LPU composite.

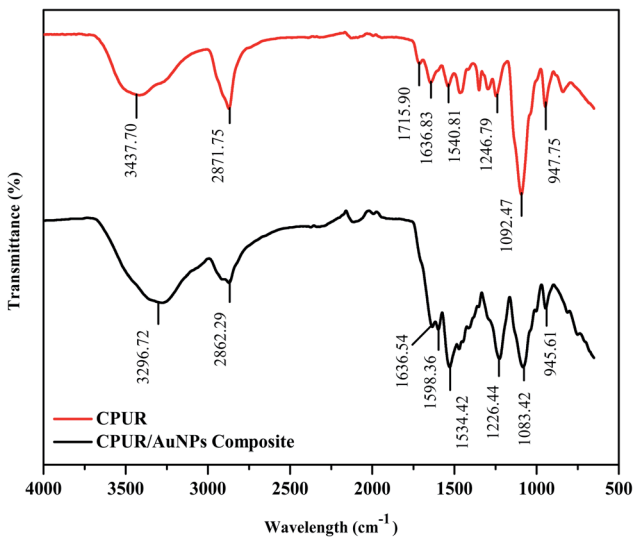

Fig. 3 FTIR spectra of synthesized cross-linked polyurethane (CPU) and Au/CPU composite.

3.3 SEM results

SEM analysis was performed to examine the morphology of Au/LPU nano-composites (Fig. 4). At higher magnification spherical composites were clearly examined. No aggregates were formed on the addition of AuNPs in LPU as suggested by FTIR (Section 3.2). The main reason for the dispersion is that AuNPs were chemically bonded with –NH group of LPU. The surface of LPU capped with AuNPs was smooth.

3.4 XRD analysis

XRD analysis was used for the determination of crystallinity of the synthesized Au/LPU composite. Four notable Bragg's peaks were observed over the range of 2 theta from 20° to 80°. The pattern revealed diffraction peaks at 38.38°, 44.24°, 64.79°, 77.83° corresponding to (111), (200), (220) and (311) planes, respectively (Fig. 5). These peaks are specific to stabilized AuNPs demonstrating the face center cubic crystal system. The synthesized PU based composite was highly pure as no irrelevant peak has observed.

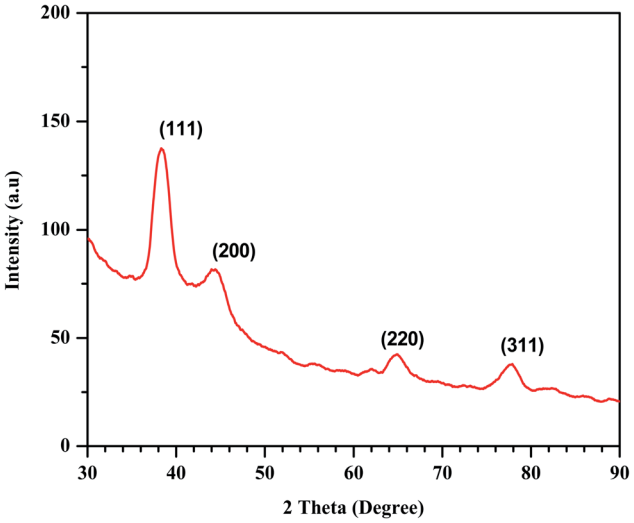

Fig. 5 XRD pattern of synthesized LPU stabilized AuNPs.

3.5 Zeta potential and dynamic light scattering (DLS) studies

Zeta Sizer (Malvern Ltd) has been used for the measurement of particle size and size distribution of Au/LPU composite and the results are shown in Fig. 6. Average size of particles is 226.4 ± 38.77 nm (*Z* average ± SD). Polydispersity index of the stabilized particles is 0.515. The zeta-potential and zeta-deviation values are −1.07 and 3.52 mV respectively. The results indicate a stable dispersion of composite.

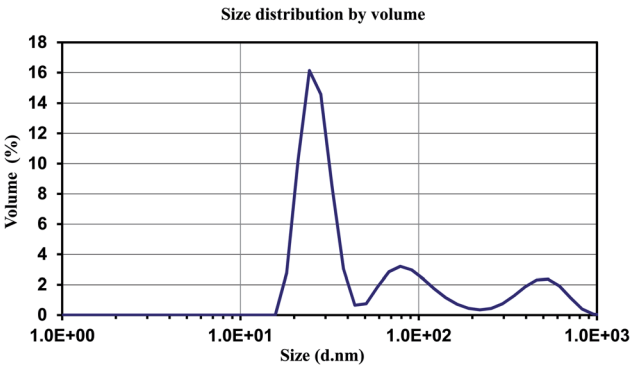

Fig. 6 Size distribution of Au/LPU composite synthesized from PU and AuNPs.

3.6 Catalytic activity of LPU and CPU based composites

Fig. 7 reveals that there was no considerable reduction of CR without composite. Absorption spectrum has shown that reduction rate was very low. Dye degradation was observed by steady fall in absorbance at 498 nm. About 30% of dye was degraded in 65 min without Au/LPU composite (Fig. 7c). By adding different amounts of composite in reaction mixture, dye was surprisingly degraded within few minutes. The dye was reduced within 6 min by using 0.3 mg of Au/LPU composite. While by using same amount of Au/CPU composite, only 30% of dye was degraded under similar conditions. These results reveal the effective catalytic activity of synthesized Au/LPU composites. Therefore, further experiments were performed preferably with Au/LPU.

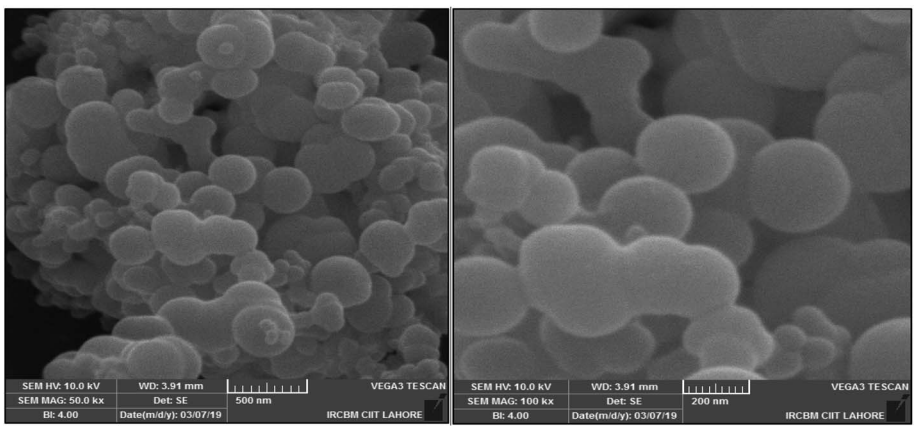

Fig. 4 SEM images of Au/LPU composite.

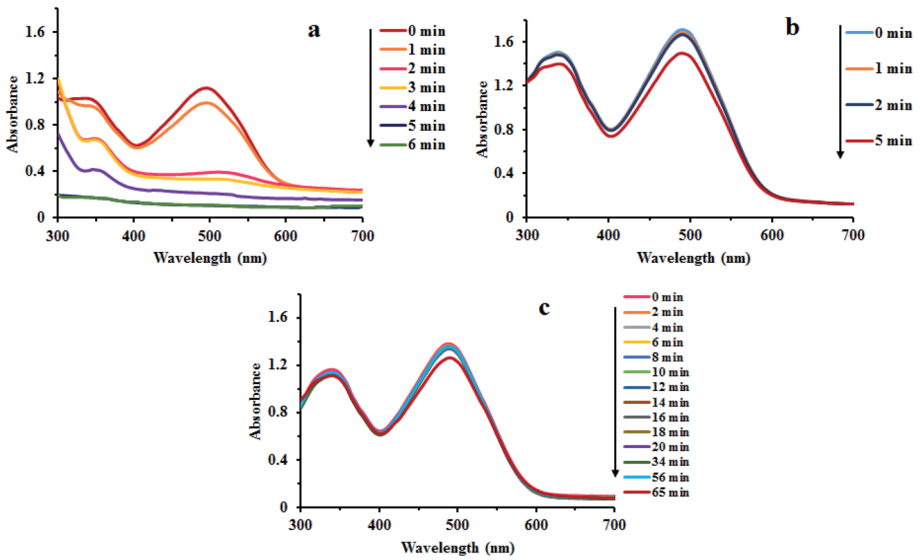

Fig. 7 Changes in the UV/Vis spectra of CR (1 mM) using: (a) $NaBH_4$ (40 mM) and 0.3 mg Au/LPU composite; (b) $NaBH_4$ (40 mM) and 0.3 mg Au/CPU composite; (c) $NaBH_4$ (40 mM) only.

The CR dye is electrophilic while BH_4^- is nucleophilic in nature. A most plausible mechanism involves the simultaneous adsorption of BH_4^- ions and CR molecules on the Au/LPU composite surfaces. Electrons from adsorbed BH_4^- ions attack on –N=N– and reduced into –HN–NH– in CR dye turning it colorless.[26,37] Au/LPU is used as a catalyst. It enhances the reduction ability of $NaBH_4$. Hence, composite has provided efficient surface for the interaction of dye molecules with BH_4^- ions. Conjugation is present in these composites, which increase the electron transfer from BH_4^- (donor) to dye (acceptor).[39] Control experiment using only sodium borohydride is too much time consuming as is obvious from Fig. 7c. Control experiments using LPU only, CPU only and their combinations with $NaBH_4$ are extensively studied in our previous report.[27] A general reaction and possible mechanism for the reduction of CR dye with Au/LPU composite has presented in Fig. 8.

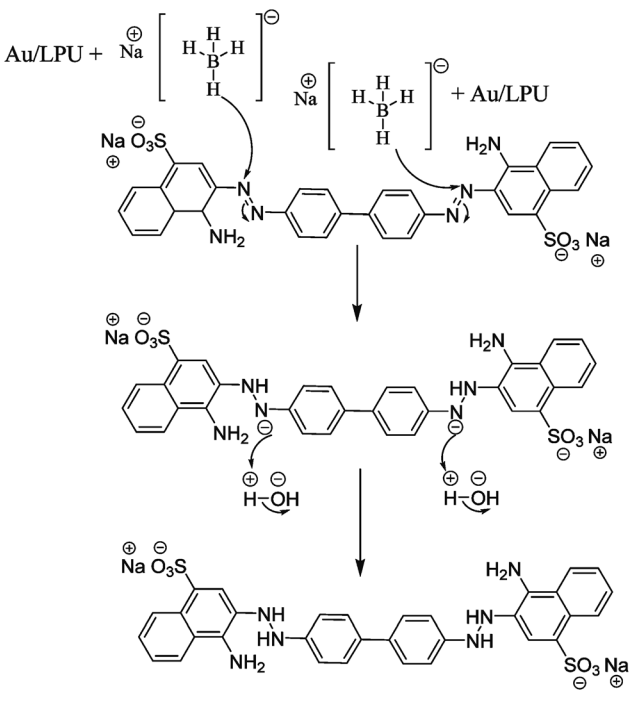

Fig. 8 Proposed mechanism for degradation of CR with Au/LPU composite and $NaBH_4$.

3.7 Effect of different reaction conditions on catalytic degradation of CR

Effect of different reaction parameters like concentration of CR dye, $NaBH_4$ and Au/LPU, time, temperature and others was tested by a series of experiments. The effect of each parameter was examined by keeping all other parameters persistent. The details of different parameters are compiled in Table 1.

3.7.1 Effect of CR dye concentration. Fig. 9 represents the degradation process with varying concentrations of CR *i.e.* 0.5 mM, 1 mM and 2 mM. There was a linear correlation between time for reduction and dye concentration. Time required for absolute reduction of dye was increased by increasing CR concentration. Most probably, at lower dye concentration, available active sites of composite for specific adsorption of BH_4^- and dye molecules were high. It led to higher adsorption rates of dye molecules and BH_4^- ions. But at higher concentration of CR, while keeping other reaction parameters constant, molecules of dye covered large number of catalyst active sites as compared to borohydride (BH_4^-) ions. Hence, number of available adsorbed BH_4^- ions for the dye degradation was decreased.[40,41]

3.7.2 $NaBH_4$ effect. The concentration of $NaBH_4$ has a profound effect on catalytic reduction of CR. Fig. 10 presents the reduction reaction with $NaBH_4$ different concentrations

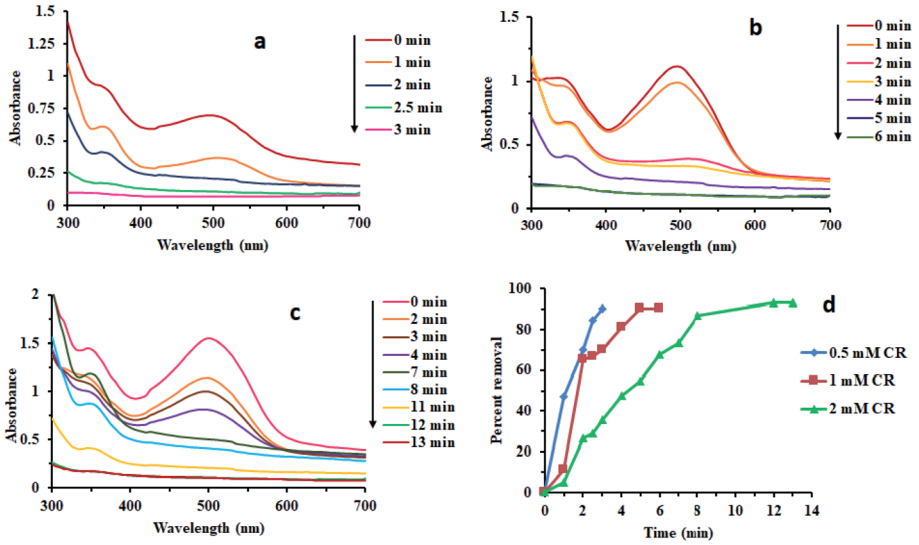

Fig. 9 UV/Vis spectra showing effect of different CR dye concentration with Au/LPU composite (0.3 mg) and $NaBH_4$ (40 mM): (a) 0.5 mM CR; (b) 1 mM CR; (c) 2 mM CR; (d) comparison of CR percent removal by using its different concentrations.

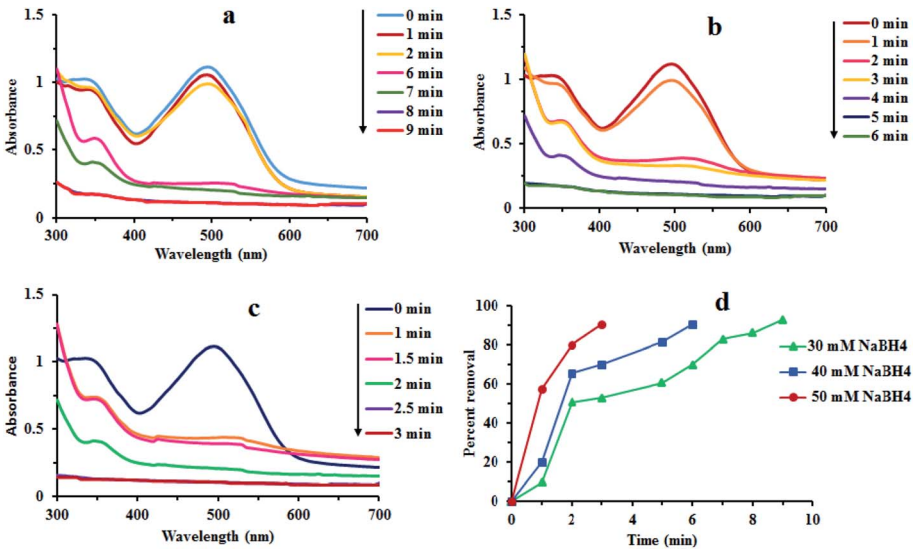

Fig. 10 UV/Vis spectra showing effect of different $NaBH_4$ concentrations on CR reduction with Au/LPU composite (0.3 mg) and CR dye (1 mM): (a) 30 mM $NaBH_4$; (b) 40 mM $NaBH_4$; (c) 50 mM $NaBH_4$; (d) comparison of percent removal of dye with different $NaBH_4$ concentrations.

while keeping all other reaction parameters constant. At higher $NaBH_4$ concentration, reduction time of dye was decreased. This relationship is appropriate as $NaBH_4$ is reducing agent, so higher concentration of it can directly promote the dye degradation reaction.[42]

3.7.3 Effect of Au/LPU composite. The amount of synthesized composite also affects CR reduction. Fig. 11 reveals the reduction reaction with different amounts of catalyst keeping all other conditions same. When the amount of catalyst increased, reduction time was decreased significantly. Reduction rate has effectively enhanced at higher doses of composite, as large number of active sites became available.[43]

3.8 Kinetic study of redox process

To find out the rate constant and order of reaction, kinetic studies of catalytic dye degradation reaction was carried out. For comparative and comprehensive investigation of kinetic variable, optimized catalytic degradation process with Au/LPU was taken against blank degradation of CR without composite. Zero, 1st and 2nd order reactions were studied. R^2 and k_{app} values for the Au/LPU composite catalyzed degradation of CR are shown in Table 2. According to the values of regression coefficient, degradation of CR solution catalyzed by composite follows 1st order kinetics as described in (Fig. 12). Apparent rate constant value for optimized catalytic CR degradation reaction by Au/LPU was 0.4715 min^{-1}.

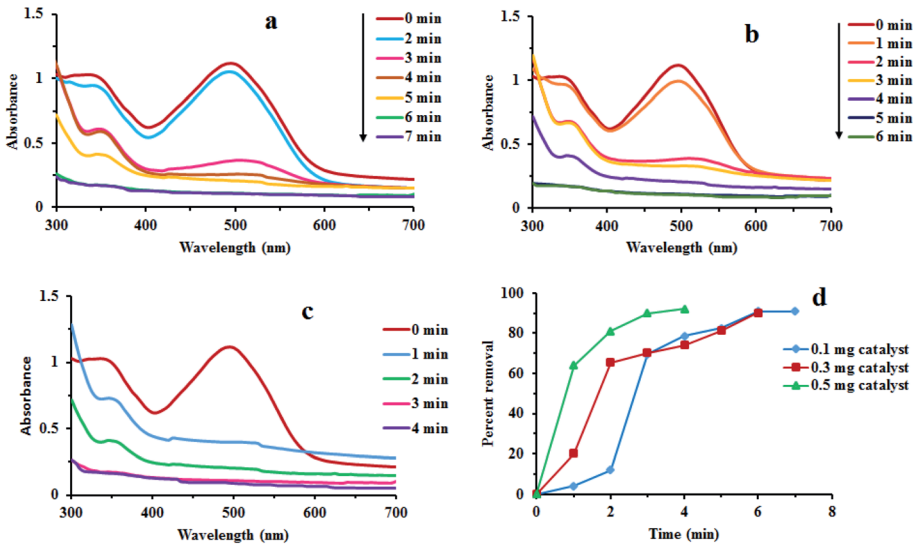

Fig. 11 UV/Vis spectra showing effect of different Au/LPU doses on CR reduction with $NaBH_4$ (40 mM) and dye (1 mM) (a) 0.1 mg Au/LPU; (b) 0.3 mg catalyst; (c) 0.5 mg catalyst; (d) comparison of percent removal of dye with different amounts of Au/LPU.

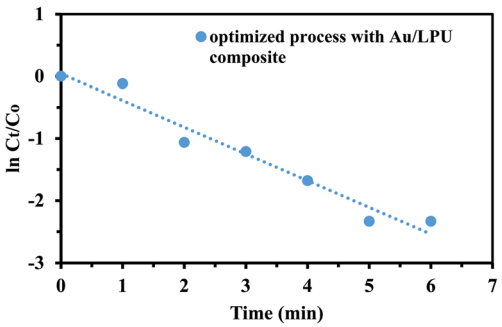

Fig. 12 Plot of $\ln(C_t/C_o)$ as a function of time (min) for CR catalytic reduction.

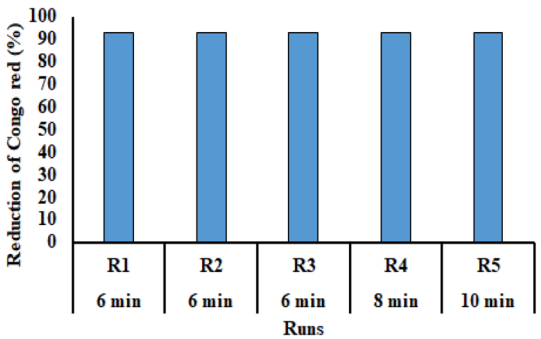

Fig. 13 Reusability studies of Au/LPU composite for degradation of CR.

3.9 Recyclability of Au/LPU composite

Recycling of Au/LPU was investigated (Fig. 13) up to five catalytic cycles for CR reduction. At the end of first run, catalyst was separated through centrifugation. In the next run, previously separated composite was instantly added in the fresh batch of dye and $NaBH_4$ solution. The reaction was monitored by UV/Vis spectrometer. After 3rd catalytic cycle, estimated time for catalytic degradation of CR was increased. The catalytic activity of Au/LPU was slightly reduced after 3rd cycle. It might be due to the loss of some active sites of composite network with successive washing and drying. Although, the composite was effective enough to show greater than 90% reduction for all other catalytic runs.

4. Conclusion

Here we report, for the first time, an eco-friendly, facile, efficient and green synthetic route to synthesize PU based gold nanocomposites. FTIR analysis confirmed the synthesis of PU based composites. SEM analysis demonstrated its structure and morphology. Spherical composites were clearly examined in

Table 2 Data of kinetic studies for reduction of CR (1 mM) with Au/LPU (0.3 mg mL^{-1}) and $NaBH_4$ (40 mM) at room temperature

Sr. no.	Kinetic model	Mathematical form of kinetic model	R^2 (regression coefficient)	K (rate constant)
1	Zero order	$C_o - C_t = kt$	0.882	0.2125 mol dm^{-3} min^{-1}
2	1st order	$\ln(C_t/C_o) = -kt$	0.963	0.4715 min^{-1}
3	2nd order	$1/C_t = kt + 1/C_o$	0.925	1.3916 mol dm^{-3} min^{-1}

SEM images. AuNPs were highly embedded in the matrix of PU. DLS studies revealed its size (226.4 nm) with polydispersity index 0.515. Au/LPU composite showed outstanding catalytic activity in reduction of CR in the presence of $NaBH_4$. The catalytic efficiency of both (Au/LPU and Au/CPU) composites was analyzed with UV/Vis technique focusing at 500 nm (maximum absorption). Composite prepared from LPU was more efficient and stable. The reason lies in linear and cross-linked structures of LPU and CPU, respectively. The flexibility is expected in linear structure of LPU while cross-linking results in rigidity of CPU. CPU forms branched chains with covalent bonds between polymer molecules. These covalent bonds are stronger than intermolecular forces that attract other polymer chains. Hence, flexible LPU made stronger interactions with AuNPs as observed by FTIR and UV-Vis spectroscopy. Ultimately, the high catalytic activity was observed with Au/LPU. CPU shows weak bonding with AuNPs. The degradation process followed 1st order kinetics. In future directions, the synthesized polymer based composites can efficiently be used for the treatment of wastewater and removal of toxic pollutants.

Conflict of interest

The authors declare "no conflict of interest" (financial or otherwise).

Acknowledgements

This work was financially supported by Higher Education Commission (HEC) Pakistan, project numbers: 8639/Punjab/NRPU/R&D/HEC/2017 and TDF-03/294. School of Chemistry, University of the Punjab is acknowledged for its support towards this project.

References

1 X. Zhao, L. Lv, B. Pan, W. Zhang, S. Zhang and Q. Zhang, *Chem. Eng. J.*, 2011, **170**, 381–394.
2 P. Joshi, S. Chakraborti, J. E. Ramirez-Vick, Z. A. Ansari, V. Shanker, P. Chakrabarti and S. P. Singh, *Colloids Surf., B*, 2012, **95**, 195–200.
3 C. -W. Chou, S. -h. Hsu and P. -H. Wang, *J. Biomed. Mater. Res., Part A*, 2008, **84**, 785–794.
4 C. O. Baker, B. Shedd, R. J. Tseng, A. A. Martinez-Morales, C. S. Ozkan, M. Ozkan, Y. Yang and R. B. Kaner, *ACS Nano*, 2011, **5**, 3469–3474.
5 Y. Li, J. T. Cox and B. Zhang, *J. Am. Chem. Soc.*, 2010, **132**, 3047–3054.
6 D. H. Wang, D. Y. Kim, K. W. Choi, J. H. Seo, S. H. Im, J. H. Park, O. O. Park and A. J. Heeger, *Angew. Chem.*, 2011, **123**, 5633–5637.
7 X.-W. Liu, F.-Y. Wang, F. Zhen and J.-R. Huang, *RSC Adv.*, 2012, **2**, 7647–7651.
8 M. Stratakis and H. Garcia, *Chem. Rev.*, 2012, **112**, 4469–4506.
9 C. A. Mirkin, R. L. Letsinger, R. C. Mucic and J. J. Storhoff, *Nature*, 1996, **382**, 607–609.
10 W. Wang, F. Wang, Y. Kang and A. Wang, *Chem. Eng. J.*, 2014, **237**, 336–343.
11 S. Hsu, C.-W. Chou and S.-M. Tseng, *Macromol. Mater. Eng.*, 2004, **289**, 1096–1101.
12 H. Zhu, M. Du, M. Zou, C. Xu, N. Li and Y. Fu, *J. Mater. Chem.*, 2012, **22**, 9301–9307.
13 M. Yadav, T. Akita, N. Tsumori and Q. Xu, *J. Mater. Chem.*, 2012, **22**, 12582–12586.
14 H. Zhu, M. Du, M. Zou, C. Xu and Y. Fu, *Dalton Trans.*, 2012, **41**, 10465–10471.
15 P. Gobbo, M. C. Biesinger and M. S. Workentin, *Chem. Commun.*, 2013, **49**, 2831–2833.
16 A. Boullanger, S. Clément, V. Mendez, S. Daniele, C. Thieuleux and A. Mehdi, *RSC Adv.*, 2013, **3**, 725–728.
17 H. Koga, E. Tokunaga, M. Hidaka, Y. Umemura, T. Saito, A. Isogai and T. Kitaoka, *Chem. Commun.*, 2010, **46**, 8567–8569.
18 R. Muszynski, B. Seger and P. V. Kamat, *J. Phys. Chem. C*, 2008, **112**, 5263–5266.
19 S. Campisi, M. Schiavoni, C. E. Chan-Thaw and A. Villa, *Catalysts*, 2016, **6**, 185–205.
20 H.-C. Kuan, C.-C. M. Ma, W.-P. Chang, S.-M. Yuen, H.-H. Wu and T.-M. Lee, *Compos. Sci. Technol.*, 2005, **65**, 1703–1710.
21 S. Hsu, C.-M. Tang and H.-J. Tseng, *J. Biomed. Mater. Res., Part A*, 2006, **79**, 759–770.
22 Y. Ganji, M. Kasra, S. S. Kordestani and M. B. Hariri, *Mater. Sci. Eng. C*, 2014, **42**, 341–349.
23 B. Finnigan, D. Martin, P. Halley, R. Truss and K. Campbell, *Polymer*, 2004, **45**, 2249–2260.
24 A. de Cuendias, R. Backov, E. Cloutet and H. Cramail, *J. Mater. Chem.*, 2005, **15**, 4196–4199.
25 J. G. Han, Y. Q. Xiang and Y. Zhu, *J. Inorg. Organomet. Polym. Mater.*, 2014, **24**, 283–290.
26 S. Hsu, C.-M. Tang and H.-J. Tseng, *Biomacromolecules*, 2007, **9**, 241–248.
27 M. Sultan, A. Javeed, M. Uroos, M. Imran, F. Jubeen, S. Nouren, N. Saleem, I. Bibi, R. Masood and W. Ahmed, *J. Hazard. Mater.*, 2018, **344**, 210–219.
28 P. Liu, H. Liu, G. Liu, K. Yao and W. Lv, *Appl. Surf. Sci.*, 2012, **258**, 9593–9598.
29 I. U. H. Bhat, M. N. K. Anwar and J. N. Appaturi, *J. Polym. Environ.*, 2019, **27**, 1475–1487.
30 M. Alle, S.-H. Lee and J.-C. Kim, *J. Mater. Sci. Technol.*, 2020, **41**, 168–177.
31 D. Xu, K. Wu, Q. Zhang, H. Hu, K. Xi, Q. Chen, X. Yu, J. Chen and X. Jia, *Polymer*, 2010, **51**, 1926–1933.
32 J. Kimling, M. Maier, B. Okenve, V. Kotaidis, H. Ballot and A. Plech, *J. Phys. Chem. B*, 2006, **110**, 15700–15707.
33 H. Maqsood, M. Uroos, R. Muazzam, S. Naz and N. Muhammad, *Int. J. Biol. Macromol.*, 2020, **164**, 1847–1857.
34 S. Phadtare, A. Kumar, V. P. Vinod, C. Dash, D. V. Palaskar, M. Rao, P. G. Shukla, S. Sivaram and M. Sastry, *Chem. Mater.*, 2003, **15**, 1944–1949.
35 S. Kumari, G. S. Chauhan and J.-H. Ahn, *Chem. Eng. J.*, 2016, **304**, 728–736.

36 V. Ribeiro da Silva, M. A. Mosiewicki, M. I. Yoshida, M. Coelho da Silva, P. M. Stefani and N. E. Marcovich, *Polym. Test.*, 2013, **32**, 438–445.
37 C.-C. Chang and C.-H. Chang, *Polym. Int.*, 2010, **59**, 910–916.
38 X. Zhou, C. Fang, W. Lei, J. Du, T. Huang, Y. Li and Y. Cheng, *Sci. Rep.*, 2016, **6**, 34574.
39 N. H. Kalwar, S. T. H. Sherazi, A. R. Khaskheli, K. R. Hallam, T. B. Scott, Z. A. Tagar, S. S. Hassan and R. A. Soomro, *Appl. Catal., A*, 2013, **453**, 54–59.
40 C. Wang, Y. Hu, C. M. Lieber and S. Sun, *J. Am. Chem. Soc.*, 2008, **130**, 8902–8903.
41 H. W. Lu, S. H. Liu, X. L. Wang, X. F. Qian, J. Yin and Z. K. Zhu, *Mater. Chem. Phys.*, 2003, **81**, 104–107.
42 M.-S. Hyun, S.-K. Kim, B. Lee, D. Peck, Y. Shul and D. Jung, *Catal. Today*, 2008, **132**, 138–145.
43 J. Fan, Y. Guo, J. Wang and M. Fan, *J. Hazard. Mater.*, 2009, **166**, 904–910.